Interaction-Induced Sign Reversal of the Orbital Magnetic Susceptibility in Chern Insulators

Ke Huang and Xiao Li*
Department of Physics, City University of Hong Kong, Kowloon, Hong Kong SAR, China

(Received 8 August 2026; accepted 27 October 2026; published 19 November 2026)

It has been well established that the orbital magnetization of interacting electrons can be simply evaluated by applying the single-particle formula to self-consistent Hartree-Fock (HF) bands. However, we show that such a procedure fails qualitatively for orbital magnetic susceptibility, especially in topological systems: in a Chern-insulating phase of twisted $MoTe_2$, the interaction-induced correction reverses the sign of the susceptibility. This result follows from an algebraic framework that solves the HF problem at finite magnetic field, where noncommuting canonical momenta obstruct a direct calculation: a *reverse Peierls substitution* maps every magnetic-translation-invariant operator to a unique bivariate function, converting the finite-field self-consistency into a function equation that can be expanded systematically in B. At first order, this yields a linear equation for the field-induced change δX of the Fock potential, leading to an intrinsically interaction-induced susceptibility in addition to a single-particle-like one. The framework reproduces the Středa formula for insulators, and an auxiliary-Hilbert-space construction carries it to periodic and moiré systems. Finite-field HF calculations in a gapped Dirac model and in the twisted $MoTe_2$ Chern insulator confirm the theory quantitatively.

DOI: 10.1103/4v66-y755

Introduction—Orbital magnetism has emerged as a central diagnostic of correlated topological phases in moiré and crystalline two-dimensional materials, aided by advances in scanning SQUID-on-tip microscopy that provide nanoscale spatial resolution and high magnetic sensitivity under cryogenic and high-field conditions [1–4]. In these systems, interaction-driven Chern insulators, orbital ferromagnets, and fractional Chern insulators—first identified through anomalous Hall transport and thermodynamic measurements [5–10]—carry orbital magnetic moments that are now directly resolved by nanoscale magnetic imaging [11–14].

The orbital magnetic susceptibility—the leading response of the magnetization to a weak field—encodes the geometry and topology of the underlying bands and, in interacting systems, the response of the self-consistent mean field itself. Moreover, local imaging of magnetization at very weak magnetic fields [15] opens up the possibility of detecting magnetic susceptibility due to orbital contributions. A predictive, gauge-invariant theory of the susceptibility for interacting electrons is therefore essential for interpreting these measurements. Indeed, we show below that interactions can reverse the sign of the orbital susceptibility of a Chern insulator in twisted $MoTe_2$ ($t$$MoTe_2$)—an effect invisible to the single-particle formula even when it is evaluated on the self-consistent Hartree-Fock bands, the very procedure that succeeds for the orbital magnetization [16,17].

For noninteracting electrons the orbital susceptibility is well understood, from the effective-Hamiltonian and semiclassical treatments of Bloch electrons in a magnetic field [18,19] to the modern theory of orbital magnetization and its geometric corrections [16,20–23]. Interactions are commonly treated within the Hartree-Fock approximation, which at zero field reduces to a self-consistent function of the Bloch momentum and—as noted above—leaves the orbital magnetization in its single-particle form once evaluated on the self-consistent quasiparticle bands [16], a statement recently shown to hold exactly in current-density-functional theory as well [17]. At finite field this Bloch-momentum description is lost: the canonical momenta no longer commute, the system discretizes into Landau levels, and a direct finite-field Hartree-Fock (HF) calculation is numerically demanding. Recent work by Kang *et al.* [24] made important progress by deriving an HF expression for the orbital magnetization and presenting a susceptibility formula written entirely in terms of the zero-field solution, numerically tested against finite-field calculations in a translation-invariant Rashba model with a contact interaction; the detailed derivation of the susceptibility, however, was deferred to a future publication, and

*Contact author: xiao.li@cityu.edu.hk

Published by the American Physical Society under the terms of the Creative Commons Attribution 4.0 International license. Further distribution of this work must maintain attribution to the author(s) and the published article's title, journal citation, and DOI.

the numerical validations in more generic systems were left open. This is part of a broader recent effort on orbital magnetism of interacting electrons, including exact response-function formulations of the magnetization [25], Luttinger-Ward-based field expansions for correlated multiband systems [26], finite-field mean-field studies of quantum Hall ferromagnets [27], and Hartree-Fock calculations of the magnetization of correlated states in twisted transition-metal dichalcogenides [28]; none of these, however, addresses the magnetic susceptibility itself.

In this Letter we address the susceptibility directly through an algebraic reformulation of the finite-field HF problem. The key object is the reverse Peierls substitution $\mathcal{R}$, which assigns to any operator commuting with the guiding-center momentum a unique bivariate function; because $\mathcal{R}$ is linear, the HF self-consistency becomes a function equation valid at both zero and finite field, and the noncommutativity enters only through a controlled $\mathcal{O}(B)$ expansion of operator products. Solving this equation to first order gives a linear equation for the change δX of the Fock potential that is efficient to solve and directly reusable. From it we obtain both $(\partial n/\partial B)_{\mu,T}|_{B=0}$—which reduces to the Středa formula for insulators—and the susceptibility $\chi^{\mathrm{HF}} = \tilde{\chi}_{\delta X} + \chi^{\mathrm{single}}_{H_0^{\mathrm{MF}}}$, cleanly separating an interaction-induced piece from a single-particle-like one. A mapping to an extended Hilbert space renders periodic and moiré systems formally translation invariant, so the same equations apply. We validate the theory against self-consistent finite-field HF in two models, extracting χ in two independent ways, and show in a $t\mathrm{MoTe}_2$ Chern insulator that the interaction correction can flip the sign of the susceptibility—demonstrating that the single-particle formula alone is qualitatively inadequate for interacting topological bands.

Hartree-Fock self-consistent equation—An interacting Hamiltonian of a 2D system with translation symmetry has the following generic form at zero magnetic field,

$$H = h(\hat{\mathbf{k}}) + \sum_{a,b} \frac{1}{2} \int \mathrm{d}^2 r \mathrm{d}^2 r' V(\mathbf{r}-\mathbf{r}') \times \psi_a^\dagger(\mathbf{r}) \psi_b^\dagger(\mathbf{r}') \psi_b(\mathbf{r}') \psi_a(\mathbf{r}), \tag{1}$$

where $V(r)$ is the interaction potential, and flavor indices a, b denote the other degrees of freedom, such as sublattices, valleys, or even nonlocal degrees of freedom, which will be elaborated on below. The single-particle Hamiltonian $h(\hat{\mathbf{k}})$ is a matrix-valued bivariate function, and its entries describe the tunneling between different degrees of freedom.

In the presence of a finite and uniform perpendicular magnetic field, the above Hamiltonian is modified by replacing the momentum operator $\hat{\mathbf{k}}$ with the canonical momentum operator $\hat{\boldsymbol{\pi}}$, whose components no longer commute, $[\hat{\pi}_x, \hat{\pi}_y] = -iB$. A bivariate function of $\hat{\boldsymbol{\pi}}$ is therefore defined only once an operator ordering is specified. Setting $\hbar = e = 1$, we adopt throughout the Weyl (symmetric) ordering,

$$h(\hat{\boldsymbol{\pi}}) = \int \mathrm{d}^2 s h^{\mathcal{F}}(\mathbf{s}) e^{i\mathbf{s}\cdot\hat{\boldsymbol{\pi}}} \tag{2}$$

with $h^{\mathcal{F}}(\mathbf{s})$ denoting the Fourier transform of $h(\mathbf{k})$. This is the standard choice for lattice models: $e^{i\mathbf{s}\cdot\hat{\boldsymbol{\pi}}}$ translates by $\mathbf{s}$ while accumulating the Peierls phase along the straight-line path joining the two endpoints, so whenever $h^{\mathcal{F}}(\mathbf{s})$ is supported on the Bravais lattice vectors, Eq. (2) is precisely the conventional Peierls substitution applied to the hopping amplitudes. Weyl ordering further maps Hermitian $h(\mathbf{k})$ to Hermitian $h(\hat{\boldsymbol{\pi}})$. All statements below—in particular the uniqueness of the reverse Peierls substitution introduced next—are understood with respect to this convention.

In the Hartree-Fock approximation, the mean-field Hamiltonian is given by (see Appendix A)

$$\hat{H}^{\mathrm{MF}} = h(\hat{\boldsymbol{\pi}}) + \hat{X}, \tag{3}$$

$$\hat{X} \equiv V_{\mathrm{MF}}[\hat{N}] \coloneqq -\int \frac{\mathrm{d}^2 q}{(2\pi)^2} \tilde{V}(q) e^{i\mathbf{q}\cdot\hat{\mathbf{r}}} \hat{N} e^{-i\mathbf{q}\cdot\hat{\mathbf{r}}}, \tag{4}$$

where $\tilde{V}(q)$ is the interaction potential in momentum space, $\hat{X}$ is the HF correction, and $\hat{N} = f_{\mathrm{FD}}(\hat{H}^{\mathrm{MF}})$ is the reduced density matrix of the HF ground state with $f_{\mathrm{FD}}(\epsilon)$ denoting the Fermi-Dirac distribution. Here, we assume (magnetic) translation symmetry, so the Hartree term becomes a constant potential and has been discarded in Eq. (3). The mean-field potential $V_{\mathrm{MF}}[\hat{N}]$ of Eq. (4) therefore contains only the Fock term, and is manifestly linear in the density matrix.

At zero field, translation symmetry guarantees that $\hat{X}$ is a function of the momentum operator. At finite field, $\hat{X}$ instead respects magnetic translation symmetry, $[\hat{X}, \hat{\mathbf{Q}}] = 0$, where $\hat{\mathbf{Q}} = \hat{\boldsymbol{\pi}} + B\hat{\mathbf{r}} \times \mathbf{z}$ is the guiding-center momentum that generates magnetic translations. The key observation is that this weaker symmetry is equally constraining: as we prove in Appendix B, any operator $\hat{A}$ commuting with $\hat{\mathbf{Q}}$ can be written as $\hat{A} = A(\hat{\boldsymbol{\pi}})$ with a unique bivariate function $A(\mathbf{k})$. Recovering $A(\mathbf{k})$ from $\hat{A}$ undoes the substitution of Eq. (2); we call this linear map the *reverse Peierls substitution*, $\mathcal{R}(\hat{A}) \coloneqq A(\mathbf{k})$. Because $\hat{H}^{\mathrm{MF}}$ and $\hat{N}$ both commute with $\hat{\mathbf{Q}}$, they are functions of $\hat{\boldsymbol{\pi}}$, and the HF correction becomes

$$V_{\mathrm{MF}}[N(\hat{\boldsymbol{\pi}})] = -\int \frac{\mathrm{d}^2 q}{(2\pi)^2} \tilde{V}(q) e^{i\mathbf{q}\cdot\hat{\mathbf{r}}} N(\hat{\boldsymbol{\pi}}) e^{-i\mathbf{q}\cdot\hat{\mathbf{r}}} = -\int \frac{\mathrm{d}^2 q}{(2\pi)^2} \tilde{V}(q) N(\hat{\boldsymbol{\pi}} - \mathbf{q}). \tag{5}$$

Applying $\mathcal{R}$ to Eq. (5) and to $\hat{N} = f_{\mathrm{FD}}(\hat{H}^{\mathrm{MF}})$ gives the self-consistent equations, valid at both zero and finite fields,

$$X(\mathbf{k}) = -\int \frac{\mathrm{d}^2 q}{(2\pi)^2} \tilde{V}(q) N(\mathbf{k}-\mathbf{q}) \equiv V_{\mathrm{MF}}[N(\mathbf{k})], \quad (6)$$

$$N(\mathbf{k}) = \mathcal{R}\{f_{\mathrm{FD}}[h(\hat{\boldsymbol{\pi}}) + X(\hat{\boldsymbol{\pi}})]\}, \quad (7)$$

where $X(\mathbf{k})$ and $N(\mathbf{k})$ are to be solved. Note that Eq. (6) is now a function equation rather than an operator equation.

Magnetic correction to the density matrix—To calculate magnetic susceptibility, we need to understand how the self-consistent solution changes with magnetic fields. Let $X_B(\mathbf{k}), N_B(\mathbf{k})$ be the self-consistent solution at magnetic field B, with mean-field Hamiltonian $H_B^{\mathrm{MF}}(\mathbf{k})$. At zero field the momentum components commute, so Eq. (7) reduces to $N_0(\mathbf{k}) = f_{\mathrm{FD}}[H_0^{\mathrm{MF}}(\mathbf{k})]$. At finite fields, (X_0, N_0) continues to satisfy Eq. (6) but fails to satisfy Eq. (7), because $\mathcal{R}[f(\hat{A})] \neq f[\mathcal{R}(\hat{A})]$ for nonlinear f and generic $\hat{A}$. The subtlety caused by the noncommutativity at finite fields can be demonstrated by considering the product of two generic functions of $\hat{\boldsymbol{\pi}}$,

$$\begin{aligned} F(\hat{\boldsymbol{\pi}})G(\hat{\boldsymbol{\pi}}) &= \int \mathrm{d}^2 s \mathrm{d}^2 s' F^{\mathcal{F}}(\mathbf{s}) G^{\mathcal{F}}(\mathbf{s}') e^{i\mathbf{s}\cdot\hat{\boldsymbol{\pi}}} e^{i\mathbf{s}'\cdot\hat{\boldsymbol{\pi}}} \\ &= \int \mathrm{d}^2 s e^{i\mathbf{s}\cdot\hat{\boldsymbol{\pi}}} \int \mathrm{d}^2 s' F^{\mathcal{F}}(\mathbf{s}-\mathbf{s}') G^{\mathcal{F}}(\mathbf{s}') e^{iB\mathbf{z}\cdot(\mathbf{s}\times\mathbf{s}')/2}. \end{aligned} \quad (8)$$

By expanding this equation to $\mathcal{O}(B^2)$, we obtain

$$\mathcal{R}[F(\hat{\boldsymbol{\pi}})G(\hat{\boldsymbol{\pi}})] = F(\mathbf{k})G(\mathbf{k}) - \frac{iB}{2}\mathbf{z}\cdot[\partial F(\mathbf{k}) \times \partial G(\mathbf{k})] + \mathcal{O}(B^2), \quad (9)$$

which yields an additional term at finite fields. Equation (9) is the $\mathcal{O}(B)$ truncation of the Moyal star product [29,30] associated with the Weyl ordering of Eq. (2); for noninteracting Bloch electrons, expansions of this type underlie the classic semiclassical theory of the susceptibility [18,19], and a related noncommutative expansion has recently been applied to the orbital magnetization of correlated electrons [26], though not to the susceptibility considered here.

The linear-in-B coefficient of the density matrix caused by noncommutativity is defined as

$$\delta N_\pi(\mathbf{k}) \coloneqq \lim_{B\to 0} \frac{\mathcal{R}[f_{\mathrm{FD}}(H_0^{\mathrm{MF}}(\hat{\boldsymbol{\pi}}))] - f_{\mathrm{FD}}[H_0^{\mathrm{MF}}(\mathbf{k})]}{B}. \quad (10)$$

It can be calculated recursively using Eq. (9), as detailed in Appendix C. A nonvanishing δN_π in turn shifts the Fock potential itself, $X_B(\mathbf{k}) = X_0(\mathbf{k}) + B\delta X(\mathbf{k}) + \mathcal{O}(B^2)$. Consequently, the total change of the density matrix is

$$N_B(\mathbf{k}) - N_0(\mathbf{k}) = B\delta N_\pi(\mathbf{k}) + B\delta N_{\delta X}(\mathbf{k}) + \mathcal{O}(B^2),$$

where

$$\delta N_{\delta X}(\mathbf{k}) = \lim_{B\to 0} \frac{f_{\mathrm{FD}}[H_0^{\mathrm{MF}}(\mathbf{k}) + B\delta X(\mathbf{k})] - f_{\mathrm{FD}}[H_0^{\mathrm{MF}}(\mathbf{k})]}{B} \quad (11)$$

can be calculated by regarding $B\delta X$ as a perturbation to H_0^{MF} (see Appendix C). Substituting the above expansions of $X_B(\mathbf{k})$ and $N_B(\mathbf{k})$ into Eq. (6) and collecting terms linear in B, we find that δX satisfies the following linear equation

$$\delta X(\mathbf{k}) = V_{\mathrm{MF}}[\delta N_\pi(\mathbf{k}) + \delta N_{\delta X}(\mathbf{k})], \quad (12)$$

which can be efficiently solved numerically. Here δN_π is a fixed source determined entirely by the zero-field solution, whereas $\delta N_{\delta X}$ is linear in δX. In our convention, quantities such as δX denote response coefficients rather than increments and carry an additional dimension of $1/B$ in their units relative to X.

Moreover, using the analytic expressions in Appendix C, we also obtain the following key result in the HF approximation,

$$\begin{aligned} \left(\frac{\partial n}{\partial B}\right)_{\mu,T}\Big|_{B=0} &= \int \frac{\mathrm{d}^2 k}{(2\pi)^2} \{\mathrm{tr}_{\mathrm{fl}}[\delta N_\pi(\mathbf{k})] + \mathrm{tr}_{\mathrm{fl}}[\delta N_{\delta X}(\mathbf{k})]\} \\ &= \sum_\alpha \int \frac{\mathrm{d}^2 k}{(2\pi)^2} (f_\alpha \Omega_\alpha - f'_\alpha m_\alpha + f'_\alpha \delta X_\alpha), \end{aligned} \quad (13)$$

where $\mathrm{tr}_{\mathrm{fl}}$ traces over the flavor indices at fixed $\mathbf{k}$, and the index α refers to $|\alpha\rangle$, the eigenstate of H_0^{MF} with eigenvalue ε_α, $f'_\alpha = f'_{\mathrm{FD}}(\varepsilon_\alpha)$, $\Omega_\alpha = -2\,\mathrm{Im}\langle\partial_x\alpha|\partial_y\alpha\rangle$ is the Berry curvature, $m_\alpha = \mathrm{Im}\langle\partial_x\alpha|(H_0^{\mathrm{MF}} - \varepsilon_\alpha)|\partial_y\alpha\rangle$ is the orbital magnetic moment, and $\delta X_\alpha = \langle\alpha|\delta X|\alpha\rangle$ is the expectation value of δX on $|\alpha\rangle$. The first two terms are the well-known result for noninteracting systems [20,22], and the HF correction produces an additional Fermi-surface term. Nonetheless, the additional term, together with the contribution from the orbital magnetic moment, vanishes for insulating states, leading to the Středa formula [31]. This proves that the HF approximation is compatible with the Středa formula for any insulating state, in agreement with previous studies [27,32].

Generalization to periodic systems—The previous discussion assumed translation symmetry; we now generalize the results to generic periodic systems. For periodic systems, the single-particle Hamiltonian $\hat{h}$ has only lattice translation symmetry, that is, $[e^{i\mathbf{R}\cdot\hat{\mathbf{Q}}}, \hat{h}] = 0$ for all real-space lattice vectors $\mathbf{R}$; equivalently, the position dependence of $\hat{h}$ has Fourier support on the set Λ of all reciprocal

lattice vectors. Hence, neither $\hat{h}$ nor $\hat{H}^{\mathrm{MF}}$ can be expressed as a function of $\hat{\boldsymbol{\pi}}$. In fact, we prove in Appendix B that operators respecting lattice translation symmetry can be expressed as functions of $\hat{\boldsymbol{\pi}}$ and $\hat{\mathbf{r}}$ with the following unique decomposition,

$$A(\hat{\boldsymbol{\pi}},\hat{\mathbf{r}})=\sum_{\mathbf{g}\in\Lambda}A_{\mathbf{g}}(\hat{\boldsymbol{\pi}})e^{i\mathbf{g}\cdot\hat{\mathbf{r}}}, \tag{14}$$

and the mean-field potential becomes

$$V_{\mathrm{MF}}[N(\hat{\boldsymbol{\pi}},\hat{\mathbf{r}})]=\mathcal{A}^{-1}\sum_{\mathbf{g}\in\Lambda}\tilde{V}(g)\mathrm{tr}_{\mathrm{phys}}[N_{\mathbf{g}}(\hat{\boldsymbol{\pi}})]e^{i\mathbf{g}\cdot\hat{\mathbf{r}}} - \int\frac{\mathrm{d}^2q}{(2\pi)^2}\tilde{V}(q)N(\hat{\boldsymbol{\pi}}-\mathbf{q},\hat{\mathbf{r}}), \tag{15}$$

where $\mathcal{A}$ is the area of the system and $\mathrm{tr}_{\mathrm{phys}}$ traces over the full physical single-particle Hilbert space, including spatial and flavor degrees of freedom. The appearance of the position operator complicates the discussion, but it can be circumvented by extending the Hilbert space.

Operators respecting lattice translation symmetry clearly form an algebra, and any set of operators sharing the same algebra essentially describes the same physics. Inspired by this concept, we introduce an extended Hilbert space $\mathcal{H}_k\otimes\mathcal{H}'$, which is a tensor product of the Hilbert space for momentum $\mathcal{H}_k$ and an auxiliary Hilbert space $\mathcal{H}'$ spanned by an orthogonal basis $\{|\mathbf{g}\rangle\}_{\mathbf{g}\in\Lambda}$. We map $\hat{A}$ in Eq. (14) to a translation-invariant operator

$$A_{\mathrm{ext}}(\hat{\boldsymbol{\pi}}):=\sum_{\mathbf{g},\mathbf{g}'\in\Lambda}A_{\mathbf{g}}(\hat{\boldsymbol{\pi}}+\mathbf{g}')|\mathbf{g}'\rangle\langle\mathbf{g}'-\mathbf{g}|, \tag{16}$$

where $A_{\mathbf{g}}(\hat{\boldsymbol{\pi}})$ are operators in $\mathcal{H}_k$. This linear map is injective and preserves the operator algebra, as shown in the Supplemental Material [33]. Therefore, any periodic operator can be mapped to a matrix-valued function of $\hat{\boldsymbol{\pi}}$, and the noncommutativity between $e^{i\mathbf{g}\cdot\hat{\mathbf{r}}}$ and $\hat{\boldsymbol{\pi}}$ is encoded in the noncommutativity between matrices. Hence, we can map the self-consistent equations to the extended Hilbert space so that the system becomes translation invariant. Moreover, as only operator algebra is used in the previous section, the result in Eq. (12) can be directly applied to the periodic case with the V_{MF} given in Eq. (15).

At zero field, $h_{\mathrm{ext}}(\mathbf{k})$ is precisely the plane-wave matrix used to solve continuum models of moiré systems. The eigenvectors of its self-consistent HF counterpart give the plane-wave coefficients of the cell-periodic Bloch states $|u_{\alpha\mathbf{k}}\rangle$, with Berry curvature $\Omega_\alpha=-2\,\mathrm{Im}\langle\partial_x u_{\alpha\mathbf{k}}|\partial_y u_{\alpha\mathbf{k}}\rangle$. In the physical Bloch description, $\mathbf{k}$ is restricted to the first Brillouin zone (BZ), whereas the extended-space representation allows $\mathbf{k}$ to range over the entire plane. The extension therefore introduces equivalent copies of the BZ, preserving the operator algebra while making continuous translational symmetry explicit. At finite fields, $h_{\mathrm{ext}}(\hat{\boldsymbol{\pi}})$ has also been explored as an alternative implementation of the Peierls substitution [34]. Truncating the auxiliary space $\mathcal{H}'$ then introduces edge states that reflect the topology of the system.

The mapping also relates the physical trace per area to a trace in the extended space [33]:

$$\frac{\mathrm{tr}_{\mathrm{phys}}[\hat{A}]}{\mathcal{A}}=\int_{\mathrm{BZ}}\frac{\mathrm{d}^2k}{(2\pi)^2}\mathrm{tr}_{\mathrm{fl}\otimes\mathcal{H}'}[A_{\mathrm{ext}}(\mathbf{k})], \tag{17}$$

where $\mathrm{tr}_{\mathrm{fl}\otimes\mathcal{H}'}$ traces over the flavor and auxiliary indices at fixed $\mathbf{k}$. Applying this identity to the product of the periodic single-particle density operator and a periodic observable allows its expectation value per area to be evaluated by integrating over one BZ in the extended-space representation. This applies both to the density response and to the magnetic responses discussed in the following section. The corresponding density-response formula for periodic systems, analogous to Eq. (13), is derived in Supplemental Material [33]. At $T=0$, with fixed μ in a gap that remains open under an infinitesimal field, the terms proportional to f'_α in the periodic density-response formula also vanish, giving

$$\left(\frac{\partial n}{\partial B}\right)_{\mu,T}\Big|_{B=0,T=0}=\sum_{\alpha\in\mathrm{occ}}\int_{\mathrm{BZ}}\frac{\mathrm{d}^2k}{(2\pi)^2}\Omega_\alpha(\mathbf{k})=\frac{C_{\mathrm{occ}}}{2\pi}. \tag{18}$$

Here C_{occ} is the total Chern number of the occupied HF bands. This is the density form of the Středa relation in our convention $\hbar=e=1$.

Magnetic susceptibility—We now discuss how the HF correction δX affects the magnetic susceptibility. Magnetic susceptibility is the rate of change of magnetization, and magnetization in the HF theory is known to have a form identical to the single-particle magnetization at both zero and finite fields [16,20–22]. Moreover, the single-particle magnetization at finite fields can be expanded in terms of B,

$$M^{\mathrm{single}}_{H(\hat{\boldsymbol{\pi}})}=M^{\mathrm{single}}_{H(\hat{\mathbf{k}})}+B\chi^{\mathrm{single}}_{H(\hat{\mathbf{k}})}+\mathcal{O}(B^2), \tag{19}$$

where $M^{\mathrm{single}}_{H(\hat{\boldsymbol{\pi}})}$ and $M^{\mathrm{single}}_{H(\hat{\mathbf{k}})}$ are respectively the single-particle magnetizations of $H(\hat{\boldsymbol{\pi}})$ and $H(\hat{\mathbf{k}})$, and $\chi^{\mathrm{single}}_{H(\hat{\mathbf{k}})}$ is the single-particle susceptibility of $H(\hat{\mathbf{k}})$ [23,35]. Hence, the HF magnetization becomes

$$\begin{aligned}M^{\mathrm{HF}}_B&=M^{\mathrm{single}}_{H^{\mathrm{MF}}_B(\hat{\boldsymbol{\pi}})}=M^{\mathrm{single}}_{H^{\mathrm{MF}}_B(\hat{\mathbf{k}})}+B\chi^{\mathrm{single}}_{H^{\mathrm{MF}}_B(\hat{\mathbf{k}})}+\mathcal{O}(B^2)\\&=M^{\mathrm{single}}_{H^{\mathrm{MF}}_0(\hat{\mathbf{k}})}+B\tilde{\chi}_{\delta X}+B\chi^{\mathrm{single}}_{H^{\mathrm{MF}}_0(\hat{\mathbf{k}})}+\mathcal{O}(B^2),\end{aligned} \tag{20}$$

where $B\tilde{\chi}_{\delta X}$ describes the change of magnetization caused by the perturbation $B\delta X$ and can be calculated by first-order perturbation theory (see Appendix D); in the last term

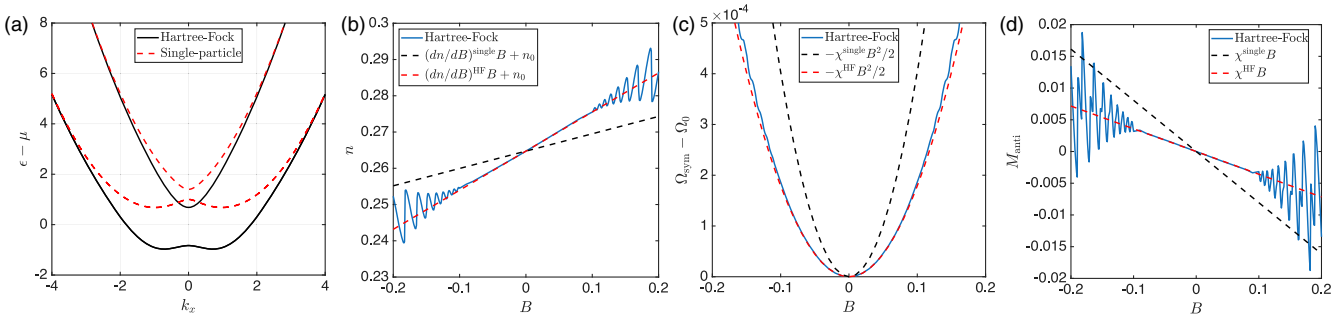


FIG. 1. HF calculations in the translation-invariant toy model. (a) HF and single-particle band structures at zero field. (b) Total density as a function of magnetic field obtained by finite-field HF calculation. (c) HF grand potential density as a function of magnetic field. (d) HF magnetization as a function of magnetic field. The red dashed lines use the full HF formula, while the black dashed lines use the single-particle formula. Here, we perform the HF calculation at a small but finite temperature $T = 0.01$ to suppress quantum oscillations.

$H_B^{\text{MF}}(\hat{\mathbf{k}})$ may be replaced by $H_0^{\text{MF}}(\hat{\mathbf{k}})$, as the correction to the subscript itself is of order B and already multiplies an explicit factor of B. Hence, we obtain the central result of the work,

$$\chi^{\text{HF}} = \lim_{B\to 0} \frac{M_B^{\text{HF}} - M_0^{\text{HF}}}{B} = \tilde{\chi}_{\delta X} + \chi^{\text{single}}_{H_0^{\text{MF}}(\hat{\mathbf{k}})}. \tag{21}$$

The additional term $\tilde{\chi}_{\delta X}$ can substantially change the susceptibility if δX is considerably large. According to Eq. (12), δX is large when δN_π is large. As $\text{tr}_{\text{fl}}[\delta N_\pi] \sim \sum_\alpha f_\alpha \Omega_\alpha$, we anticipate a large correction from this additional term if the occupied states contribute a large Berry curvature.

Numerical results—We numerically test our theory in both translation-invariant and periodic systems. We first study a translation-invariant single-particle Hamiltonian

$$h(\mathbf{k}) = k^2/(2m) + v\mathbf{k}\cdot\boldsymbol{\sigma} + \Delta\sigma_z \tag{22}$$

with a Gaussian interaction $\tilde{V}(q) = Ue^{-q^2/2\lambda^2}$. The parameters are given in Appendix E. In this system, there is a Dirac cone at $\mathbf{k} = 0$ with a small gap opened by Δ and the interaction, as shown by the HF band structure at zero field in Fig. 1(a). The occupied states have a large Berry curvature and consequently a large δX, if only the lowest band at $\mathbf{k} = 0$ is occupied. The expected correction from δX is demonstrated in Fig. 1(b), where we perform HF calculations at finite fields with fixed chemical potential $\mu = -1.2$. As the ground state is metallic, we introduce a small temperature of $T = 0.01$ to suppress quantum oscillations. The slope of the total density is accurately captured by Eq. (13), whereas the single-particle formula, the first two terms in Eq. (13), significantly deviates from the finite-field HF results. The indispensable role of δX is also highlighted by its contribution to magnetic susceptibility. We numerically verify the magnetic susceptibility by calculating symmetrized grand potential density $\Omega_{\text{sym}} = [\Omega(B) + \Omega(-B)]/2 = \Omega_0 - \chi B^2/2 + \mathcal{O}(B^4)$ in Fig. 1(c) and antisymmetrized magnetization $M_{\text{anti}} = [M(B) - M(-B)]/2 = \chi B + \mathcal{O}(B^3)$ in Fig. 1(d). Both show striking agreement between our interacting theory of magnetic susceptibility and the numerical results at finite fields. Meanwhile, the single-particle formula $\chi^{\text{single}}_{H_0^{\text{MF}}(\hat{\mathbf{k}})}$ alone cannot correctly describe the system.

Second, we study a topologically nontrivial periodic system, the continuum model of $t\text{MoTe}_2$ [36], and perform unprojected HF calculations at both zero and finite fields. We only use it as a toy model and ignore the spin and valley degrees of freedom. Moreover, we adopt the hole language rather than the electron language, so the topmost valence band of Ref. [36] becomes the lowest band of Eq. (23), with a positive effective mass. The single-particle Hamiltonian is given by

$$\hat{h} = \begin{bmatrix} \hat{k}_t^2/(2m) + V_t(\hat{\mathbf{r}}) & T(\hat{\mathbf{r}}) \\ T(\hat{\mathbf{r}})^\dagger & \hat{k}_b^2/(2m) + V_b(\hat{\mathbf{r}}) \end{bmatrix}, \tag{23}$$

where $\hat{\boldsymbol{k}}_{t/b} = \hat{\boldsymbol{k}} - \boldsymbol{\kappa}_{t/b}$ is the momentum in the top or bottom layer, $\boldsymbol{\kappa}_{t/b}$ denotes the corresponding K-valley momentum, $V_{t/b}(\hat{\mathbf{r}})$ describe the moiré potentials in the top and bottom MoTe_2 layers, and $T(\hat{\mathbf{r}})$ describes the tunneling between the two layers. Furthermore, we consider the dual-gate screened Coulomb potential $\tilde{V}(q) = e^2 \tanh(qd)/(2\epsilon\epsilon_0 q)$ with $d = 3$ nm and $\epsilon = 25$. The other parameters and a detailed description of the model are given in Appendix E. The lowest band of the single-particle system has Chern number $C = -1$, and we fix $\mu = -23$ meV so that the HF ground state at zero field is a Chern insulator, as shown by the HF band structure in Fig. 2(a). In Fig. 2(b), we calculate the total density of the HF ground state as a function of magnetic field, which exactly follows the Středa formula as we proved. We emphasize that in spite of the theoretical equivalence, the conventional Peierls substitution [37] is more suitable for numerical HF calculations than the open-space one [34], because the conventional one has no

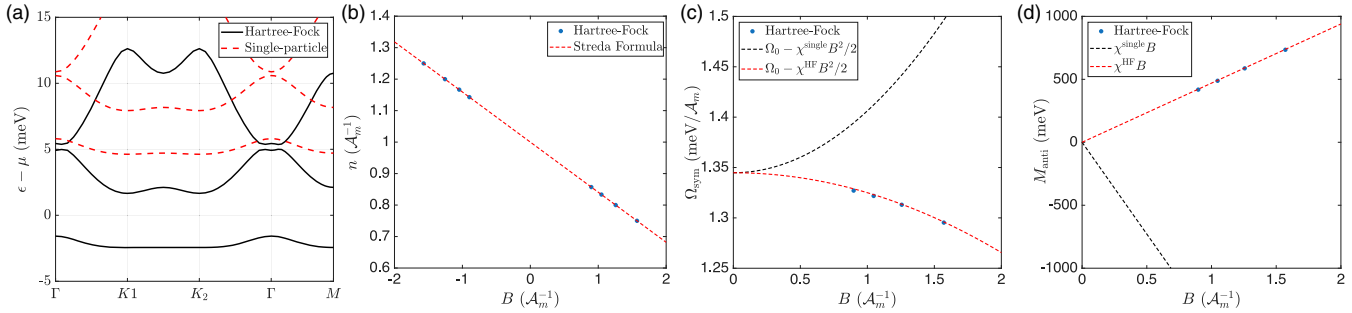


FIG. 2. HF calculations in the periodic toy model. (a) HF and single-particle band structures at zero field. (b) Total density as a function of magnetic field obtained by finite-field HF calculation. Here, $\mathcal{A}_m$ is the area of the moiré unit cell. (c) Symmetrized grand potential density Ω_{sym} as a function of magnetic field: the single-particle formula (black dashed) predicts the wrong curvature, i.e., the wrong sign of χ. (d) Antisymmetrized magnetization: the finite-field HF data fall on the line of the full HF susceptibility χ^{HF} (red dashed), while the single-particle slope (black dashed) has the opposite sign.

edge states. Note that while δX does not contribute to $(\partial n/\partial B)_{\mu,T}|_{B=0,T=0}$ for insulators, it can still provide a substantial correction to the magnetic susceptibility. In Fig. 2(c), we calculate the symmetrized grand potential Ω_{sym}, which agrees with χ^{HF} in Eq. (21) remarkably well. In contrast, $\chi^{\text{single}}_{H_0^{\text{MF}}(\hat{\mathbf{k}})}$ alone cannot even give the correct sign of the magnetic susceptibility. The accuracy of our theory is better presented by the antisymmetrized magnetization, which has better numerical precision than energy, because χ^{HF} is a second-order correction to energy but a first-order correction to magnetization. As shown in Fig. 2(d), the magnetization falls perfectly on the theoretical line of χ^{HF}. By contrast, the single-particle formula $\chi^{\text{single}}_{H_0^{\text{MF}}(\hat{\mathbf{k}})}$ is far from the actual magnetization.

Summary and outlook—We have developed an algebraic theory of the Hartree-Fock response to a magnetic field: the reverse Peierls substitution converts the finite-field self-consistency into a function equation continuously connected to zero field, whose $\mathcal{O}(B)$ expansion yields a linear equation for the field-induced Fock correction δX; periodic and moiré systems enter as translation-invariant ones in an extended Hilbert space. The $t\text{MoTe}_2$ calculation carries a direct experimental message: for interacting Chern bands, the single-particle susceptibility evaluated on the self-consistent bands can fail even in sign, so the interaction term $\tilde{\chi}_{\delta X}$ is indispensable for interpreting magnetic and thermodynamic measurements of moiré Chern insulators [8,11,13]. The framework we developed is gauge invariant by construction and systematically extendable: Eq. (12) generalizes to arbitrary order in B, giving immediate access to nonlinear magnetic responses.

Acknowledgments—This work is supported by the Research Grants Council of Hong Kong (Grants No. CityU 11304823, No. CityU 11312825, No. C7012-21G, and No. C7015-24G) and City University of Hong Kong (Project No. 9610428). Open Access made possible with partial support from the Open Access Publishing Fund of the City University of Hong Kong.

Data availability—There are no publicly available research data or software supporting this manuscript. Requests for further information or data should be sent to the authors.

[1] A. Finkler, D. Vasyukov, Y. Segev, L. Ne'eman, E. O. Lachman, M. L. Rappaport, Y. Myasoedov, E. Zeldov, and M. E. Huber, Scanning superconducting quantum interference device on a tip for magnetic imaging of nanoscale phenomena, Rev. Sci. Instrum. **83**, 073702 (2012).

[2] D. Vasyukov, Y. Anahory, L. Embon, D. Halbertal, J. Cuppens, L. Ne'eman, A. Finkler, Y. Segev, Y. Myasoedov, M. L. Rappaport, M. E. Huber, and E. Zeldov, A scanning superconducting quantum interference device with single electron spin sensitivity, Nat. Nanotechnol. **8**, 639 (2013).

[3] Y. Anahory, H. R. Naren, E. O. Lachman, S. Buhbut Sinai, A. Uri, L. Embon, E. Yaakobi, Y. Myasoedov, M. E. Huber, R. Klajn, and E. Zeldov, SQUID-on-tip with single-electron spin sensitivity for high-field and ultra-low temperature nanomagnetic imaging, Nanoscale **12**, 3174 (2020).

[4] H. Zhou, N. Auerbach, I. Roy, M. Bocarsly, M. E. Huber, B. Barick, A. Pariari, M. Hücker, Z. S. Lim, A. Ariando, A. I. Berdyugin, N. Xin, M. Rappaport, Y. Myasoedov, and E. Zeldov, Scanning SQUID-on-tip microscope in a top-loading cryogen-free dilution refrigerator, Rev. Sci. Instrum. **94**, 053706 (2023).

[5] A. L. Sharpe, E. J. Fox, A. W. Barnard, J. Finney, K. Watanabe, T. Taniguchi, M. A. Kastner, and D. Goldhaber-Gordon, Emergent ferromagnetism near three-quarters filling in twisted bilayer graphene, Science **365**, 605 (2019).

[6] M. Serlin, C. L. Tschirhart, H. Polshyn, Y. Zhang, J. Zhu, K. Watanabe, T. Taniguchi, L. Balents, and A. F. Young, Intrinsic quantized anomalous Hall effect in a moiré heterostructure, Science **367**, 900 (2020).

[7] J. Cai, E. Anderson, C. Wang, X. Zhang, X. Liu, W. Holtzmann, Y. Zhang, F. Fan, T. Taniguchi, K. Watanabe,

Y. Ran, T. Cao, L. Fu, D. Xiao, W. Yao, and X. Xu, Signatures of fractional quantum anomalous Hall states in twisted $MoTe_2$, Nature (London) **622**, 63 (2023).

[8] Y. Zeng, Z. Xia, K. Kang, J. Zhu, P. Knüppel, C. Vaswani, K. Watanabe, T. Taniguchi, K. F. Mak, and J. Shan, Thermodynamic evidence of fractional Chern insulator in moiré $MoTe_2$, Nature (London) **622**, 69 (2023).

[9] H. Park, J. Cai, E. Anderson, Y. Zhang, J. Zhu, X. Liu, C. Wang, W. Holtzmann, C. Hu, Z. Liu, T. Taniguchi, K. Watanabe, J.-H. Chu, T. Cao, L. Fu, W. Yao, C.-Z. Chang, D. Cobden, D. Xiao, and X. Xu, Observation of fractionally quantized anomalous Hall effect, Nature (London) **622**, 74 (2023).

[10] F. Xu, Z. Sun, T. Jia, C. Liu, C. Xu, C. Li, Y. Gu, K. Watanabe, T. Taniguchi, B. Tong, J. Jia, Z. Shi, S. Jiang, Y. Zhang, X. Liu, and T. Li, Observation of integer and fractional quantum anomalous Hall effects in twisted bilayer $MoTe_2$, Phys. Rev. X **13**, 031037 (2023).

[11] C. L. Tschirhart, M. Serlin, H. Polshyn, A. Shragai, Z. Xia, J. Zhu, Y. Zhang, K. Watanabe, T. Taniguchi, M. E. Huber, and A. F. Young, Imaging orbital ferromagnetism in a moiré Chern insulator, Science **372**, 1323 (2021).

[12] S. Grover, M. Bocarsly, A. Uri, P. Stepanov, G. Di Battista, I. Roy, J. Xiao, A. Y. Meltzer, Y. Myasoedov, K. Pareek, K. Watanabe, T. Taniguchi, B. Yan, A. Stern, E. Berg, D. K. Efetov, and E. Zeldov, Chern mosaic and Berry-curvature magnetism in magic-angle graphene, Nat. Phys. **18**, 885 (2022).

[13] E. Redekop, C. Zhang, H. Park, J. Cai, E. Anderson, O. Sheekey, T. Arp, G. Babikyan, S. Salters, K. Watanabe, T. Taniguchi, M. E. Huber, X. Xu, and A. F. Young, Direct magnetic imaging of fractional Chern insulators in twisted $MoTe_2$, Nature (London) **635**, 584 (2024).

[14] N. Auerbach, S. Dutta, M. Uzan, Y. Vituri, Y. Zhou, A. Y. Meltzer, S. Grover, T. Holder, P. Emanuel, M. E. Huber, Y. Myasoedov, K. Watanabe, T. Taniguchi, Y. Oreg, E. Berg, and E. Zeldov, Isospin magnetic texture and intervalley exchange interaction in rhombohedral tetralayer graphene, Nat. Phys. **21**, 1765 (2025).

[15] H. Zhou, N. Auerbach, M. Uzan, Y. Zhou, N. Banu, W. Zhi, M. E. Huber, K. Watanabe, T. Taniguchi, Y. Myasoedov, B. Yan, and E. Zeldov, Imaging quantum oscillations and millitesla pseudomagnetic fields in graphene, Nature (London) **624**, 275 (2023).

[16] J. Shi, G. Vignale, D. Xiao, and Q. Niu, Quantum theory of orbital magnetization and its generalization to interacting systems, Phys. Rev. Lett. **99**, 197202 (2007).

[17] G. Vignale, J. Shi, D. Xiao, and Q. Niu, Ward identities and orbital magnetization in current density functional theory, arXiv:2605.14336.

[18] E. I. Blount, Bloch electrons in a magnetic field, Phys. Rev. **126**, 1636 (1962).

[19] L. M. Roth, Semiclassical theory of magnetic energy levels and magnetic susceptibility of Bloch electrons, Phys. Rev. **145**, 434 (1966).

[20] D. Xiao, J. Shi, and Q. Niu, Berry phase correction to electron density of states in solids, Phys. Rev. Lett. **95**, 137204 (2005).

[21] T. Thonhauser, D. Ceresoli, D. Vanderbilt, and R. Resta, Orbital magnetization in periodic insulators, Phys. Rev. Lett. **95**, 137205 (2005).

[22] D. Xiao, M.-C. Chang, and Q. Niu, Berry phase effects on electronic properties, Rev. Mod. Phys. **82**, 1959 (2010).

[23] Y. Gao, S. A. Yang, and Q. Niu, Geometrical effects in orbital magnetic susceptibility, Phys. Rev. B **91**, 214405 (2015).

[24] J. Kang, M. Wang, and O. Vafek, Orbital magnetization and magnetic susceptibility of interacting electrons, arXiv:2509.20626.

[25] X. Chen and Z.-D. Song, Orbital magnetization of interacting electrons, arXiv:2602.02478.

[26] M. Ye, A quantum many-body approach for orbital magnetism in correlated multiband electron systems, arXiv:2601.14372.

[27] C. Huang, Orbital magnetization from uniform and periodic magnetic fields, arXiv:2605.26889.

[28] X. Liu, C. Wang, H. Chen, X.-W. Zhang, T. Cao, and D. Xiao, Orbital magnetization of correlated states in twisted bilayer transition metal dichalcogenides, Phys. Rev. Lett. **136**, 166606 (2026).

[29] H. J. Groenewold, On the principles of elementary quantum mechanics, Physica (Amsterdam) **12**, 405 (1946).

[30] J. E. Moyal, Quantum mechanics as a statistical theory, Proc. Cambridge Philos. Soc. **45**, 99 (1949).

[31] P. Středa, Theory of quantised Hall conductivity in two dimensions, J. Phys. C **15**, L717 (1982).

[32] J. Zhu and C. Huang, Orbital magnetization and Středa formula of interacting electrons in the mean-field approximation, Phys. Rev. B **113**, 205114 (2026).

[33] See Supplemental Material at http://link.aps.org/supplemental/10.1103/4v66-y755 for the algebra-preserving extended-space representation, the trace correspondence, and the Středa formula in periodic systems.

[34] B. Lian, F. Xie, and B. A. Bernevig, Open momentum space method for the Hofstadter butterfly and the quantized Lorentz susceptibility, Phys. Rev. B **103**, L161405 (2021).

[35] A. Raoux, F. Piéchon, J.-N. Fuchs, and G. Montambaux, Orbital magnetism in coupled-bands models, Phys. Rev. B **91**, 085120 (2015).

[36] F. Wu, T. Lovorn, E. Tutuc, I. Martin, and A. H. MacDonald, Topological insulators in twisted transition metal dichalcogenide homobilayers, Phys. Rev. Lett. **122**, 086402 (2019).

[37] X. Wang and O. Vafek, Theory of correlated Chern insulators in twisted bilayer graphene, Phys. Rev. X **14**, 021042 (2024).

End Matter

Appendix A: Hartree-Fock self-consistent equation—In this appendix, we derive the HF self-consistent equation. In the Hartree-Fock approximation, the interaction becomes Hartree and Fock terms, yielding the following mean-field Hamiltonian

$$\hat{H}^{\mathrm{MF}} = \hat{h} + \int \mathrm{d}^2 r \mathrm{d}^2 r' V(\mathbf{r}-\mathbf{r}')\langle n(\mathbf{r}')\rangle n(\mathbf{r}) - \sum_{a,b}\int \mathrm{d}^2 r \mathrm{d}^2 r' V(\mathbf{r}-\mathbf{r}')\langle \psi_a^\dagger(\mathbf{r}')\psi_b(\mathbf{r})\rangle \psi_b^\dagger(\mathbf{r})\psi_a(\mathbf{r}'), \tag{A1}$$

where the second and third terms are, respectively, the Hartree and Fock terms, and $n(\mathbf{r}) = \sum_a \psi_a^\dagger(\mathbf{r})\psi_a(\mathbf{r})$ is the total density. If the ground state has continuous or discrete translation symmetry, the Hartree term becomes

$$\text{Hartree term} = \mathcal{A}^{-1}\sum_{\mathbf{g}\in\Lambda}\tilde{V}(g)e^{i\mathbf{g}\cdot\hat{\mathbf{r}}}\langle e^{-i\mathbf{g}\cdot\hat{\mathbf{r}}}\rangle, \tag{A2}$$

where $\Lambda = \{\mathbf{0}\}$ for translation-invariant systems, and Λ is the set of all reciprocal vectors for periodic systems. As the $\mathbf{g}=\mathbf{0}$ contribution is always canceled by the positive charge background, we set $\tilde{V}(q=0)=0$ henceforth.

The Fock term can be simplified as

$$\begin{aligned}\text{Fock term} &= -\sum_{a,b}\int \frac{\mathrm{d}^2 q}{(2\pi)^2}\tilde{V}(q)\int \mathrm{d}^2 r \mathrm{d}^2 r' e^{i\mathbf{q}\cdot(\mathbf{r}-\mathbf{r}')} \times \langle \psi_a^\dagger(\mathbf{r}')\psi_b(\mathbf{r})\rangle \psi_b^\dagger(\mathbf{r})\psi_a(\mathbf{r}') \\ &= -\int \frac{\mathrm{d}^2 q}{(2\pi)^2}\tilde{V}(q)e^{i\mathbf{q}\cdot\hat{\mathbf{r}}}\hat{N}e^{-i\mathbf{q}\cdot\hat{\mathbf{r}}},\end{aligned} \tag{A3}$$

because in first-quantized notation, we have

$$\sum_{a,b}\int \mathrm{d}^2 r \mathrm{d}^2 r' \langle \psi_a^\dagger(\mathbf{r})\psi_b(\mathbf{r}')\rangle \psi_b^\dagger(\mathbf{r}')\psi_a(\mathbf{r}) = \sum_{a,b}\int \mathrm{d}^2 r \mathrm{d}^2 r' \langle \mathbf{r}a|\hat{N}|\mathbf{r}'b\rangle |\mathbf{r}a\rangle\langle \mathbf{r}'b| = \hat{N}, \tag{A4}$$

where $|\mathbf{r}a\rangle$ is a position eigenstate with flavor a. Substituting it into Eq. (A3), we obtain the result in the main text.

Appendix B: Reverse Peierls substitution—In this appendix, we prove the existence and uniqueness of the reverse Peierls substitution. Because the canonical momenta $\hat{\boldsymbol{\pi}}$ commute with the guiding-center momenta $\hat{\mathbf{Q}}$, the Hilbert space can be decomposed into the tensor product of two Landau-level systems. In the symmetric gauge, the canonical momenta generate the physical Landau levels, while the guiding-center momenta generate the angular momentum. The Peierls substitution is a Weyl transform, whose unique inverse is the Wigner map. Thus, for any operator $\hat{A}$, there exists a function $f(\mathbf{s},\mathbf{s}')$ satisfying

$$\begin{aligned}\hat{A} &= \int \mathrm{d}^2 s \mathrm{d}^2 s' f(\mathbf{s},\mathbf{s}')e^{i\mathbf{s}\cdot\hat{\boldsymbol{\pi}}+i\mathbf{s}'\cdot\hat{\mathbf{Q}}} \\ &= \int \mathrm{d}^2 s \mathrm{d}^2 s' \tilde{f}(\mathbf{s},\mathbf{s}')e^{i\mathbf{s}\cdot\hat{\boldsymbol{\pi}}}e^{i\mathbf{s}'\cdot\hat{\mathbf{r}}}\end{aligned} \tag{B1}$$

with $\tilde{f}(\mathbf{s},\mathbf{s}') = f(\mathbf{s}-\mathbf{s}'\times\mathbf{z}/B, \mathbf{s}'\times\mathbf{z}/B)e^{-i\mathbf{s}\cdot\mathbf{s}'/2}/B^2$.

If $\hat{A}$ is translation invariant, $\hat{A}$ is only a function of $\boldsymbol{\pi}$ and $f(\mathbf{s},\mathbf{s}')$ has support only at $\mathbf{s}'=\mathbf{0}$. If $\hat{A}$ is periodic, then $\tilde{f}(\mathbf{s},\mathbf{s}') = \tilde{f}(\mathbf{s},\mathbf{s}')e^{i\mathbf{s}'\cdot\mathbf{R}}$ for all lattice vectors $\mathbf{R}$ in real space. Therefore, $\tilde{f}(\mathbf{s},\mathbf{s}')$ has support only at $\mathbf{s}'=\mathbf{g}\in\Lambda$, and correspondingly, we have

$$\hat{A} = \sum_{\mathbf{g}\in\Lambda}\int \mathrm{d}^2 s \tilde{f}(\mathbf{s},\mathbf{g})e^{i\mathbf{s}\cdot\hat{\boldsymbol{\pi}}}e^{i\mathbf{g}\cdot\hat{\mathbf{r}}} = \sum_{\mathbf{g}\in\Lambda}A_{\mathbf{g}}(\hat{\boldsymbol{\pi}})e^{i\mathbf{g}\cdot\hat{\mathbf{r}}}, \tag{B2}$$

where $A_{\mathbf{g}}(\hat{\boldsymbol{\pi}}) = \int \mathrm{d}^2 s \tilde{f}(\mathbf{s},\mathbf{g})e^{i\mathbf{s}\cdot\hat{\boldsymbol{\pi}}}$.

Appendix C: Density change at finite magnetic fields—In this appendix, we will use Eq. (9) to derive the analytic expressions for δN_π and $\delta N_{\delta X}$, which are

$$\begin{aligned}\delta N_\pi(\mathbf{k}) &= -\frac{i}{2}\sum_{\alpha,\beta}|\alpha\rangle\langle\beta|\sum_\gamma K_{f_{\mathrm{FD}}}(\varepsilon_\alpha,\varepsilon_\gamma,\varepsilon_\beta)\mathbf{z}\cdot(\mathbf{v}_{\alpha\gamma}\times\mathbf{v}_{\gamma\beta}), \\ \delta N_{\delta X}(\mathbf{k}) &= \sum_{\varepsilon_\alpha\neq\varepsilon_\beta}|\alpha\rangle\langle\beta|\frac{f_\alpha - f_\beta}{\varepsilon_\alpha-\varepsilon_\beta}\langle\alpha|\delta X|\beta\rangle + \sum_{\varepsilon_\alpha=\varepsilon_\beta}|\alpha\rangle\langle\beta|f'_\alpha\langle\alpha|\delta X|\beta\rangle,\end{aligned} \tag{C1}$$

where $|\alpha\rangle$ is the eigenstate of $H_0^{\mathrm{MF}}(\mathbf{k})$ with eigenvalue ε_α, $\mathbf{v}_{\alpha\beta} = \langle\alpha|\partial H_0^{\mathrm{MF}}(\mathbf{k})|\beta\rangle$, $f_\alpha = f_{\mathrm{FD}}(\varepsilon_\alpha)$, and for a univariate function f and $a_1\neq a_2\neq a_3\neq a_1$, we define

$$\begin{aligned}K_f(a_1,a_2,a_3) &= \frac{1}{2}\sum_{\sigma\in S_3}\frac{f(a_{\sigma(1)})}{(a_{\sigma(2)}-a_{\sigma(1)})(a_{\sigma(3)}-a_{\sigma(1)})} \\ K_f(a_2,a_1,a_1) &= K_f(a_1,a_2,a_1) = K_f(a_1,a_1,a_2) \\ &= \frac{f(a_2)-f(a_1)}{(a_2-a_1)^2} - \frac{f'(a_1)}{a_2-a_1} \\ K_f(a_1,a_1,a_1) &= f''(a_1)/2,\end{aligned} \tag{C2}$$

with S_3 denoting the permutation group on three elements. Following Eq. (C4), both sums in $\delta N_{\delta X}$ are keyed on eigenvalues rather than state labels, so that

degenerate pairs $\alpha \neq \beta$ enter the second sum and $\delta N_{\delta X}$ is basis independent within a multiplet.

One can inductively prove for all integers $a \geq 2$ that

$$\begin{aligned}
&\lim_{B\to 0}\frac{\langle\alpha|\mathcal{R}[H(\hat{\boldsymbol{\pi}})^a]-H^a|\beta\rangle}{B}\\
&=\lim_{B\to 0}\frac{\langle\alpha|(\mathcal{R}[H(\hat{\boldsymbol{\pi}})^{a-1}]-H^{a-1})H|\beta\rangle}{B}-\frac{i}{2}\mathbf{z}\cdot\langle\alpha|\partial H^{a-1}\times\mathbf{v}|\beta\rangle\\
&=-\frac{i}{2}\sum_{\gamma}\mathbf{z}\cdot(\mathbf{v}_{\alpha\gamma}\times\mathbf{v}_{\gamma\beta})\sum_{m=0}^{a-2}\sum_{n=0}^{a-m-2}\varepsilon_\alpha^m\varepsilon_\gamma^n\varepsilon_\beta^{a-m-n-2}\\
&=-\frac{i}{2}\sum_{\gamma}\mathbf{z}\cdot(\mathbf{v}_{\alpha\gamma}\times\mathbf{v}_{\gamma\beta})K_{x^a}(\varepsilon_\alpha,\varepsilon_\gamma,\varepsilon_\beta),
\end{aligned}\tag{C3}$$

where all $\mathbf{k}$ arguments and the superscript and subscript of H_0^{MF} are omitted for convenience, $\mathbf{v}=\partial H$, and the last equality is obtained by calculating the sum of the geometric sequence. Moreover, as $K_{x^0}(a_1,a_2,a_3)=K_{x^1}(a_1,a_2,a_3)=0$, Eq. (C3) also holds for $a=0,1$. Hence, Eq. (C3) also holds if the power function x^a is replaced with any polynomial $P(x)$. Additionally, because functions can generally be approximated by polynomials, Eq. (C3) also holds if the power function x^a is replaced with the Fermi-Dirac distribution, which gives the δN_π in Eq. (C1).

Similarly, it is easy to prove that for polynomials $P(x)$

$$\lim_{B\to 0}\frac{\langle\alpha|P(H+B\delta X)-P(H)|\beta\rangle}{B}=\begin{cases}\frac{P(\varepsilon_\alpha)-P(\varepsilon_\beta)}{\varepsilon_\alpha-\varepsilon_\beta}\langle\alpha|\delta X|\beta\rangle & \text{if } \varepsilon_\alpha\neq\varepsilon_\beta,\\ P'(\varepsilon_\alpha)\langle\alpha|\delta X|\beta\rangle & \text{if } \varepsilon_\alpha=\varepsilon_\beta.\end{cases}\tag{C4}$$

By the same argument, we can replace the polynomial $P(x)$ with the Fermi-Dirac distribution $f_{\mathrm{FD}}(x)$.

Appendix D: Calculation of $\tilde{\chi}_{\delta X}$—In this appendix, we derive the formula for $\tilde{\chi}_{\delta X}$. The mean-field magnetization is given by

$$M^{\mathrm{HF}}=\sum_\alpha\int\frac{\mathrm{d}^2k}{(2\pi)^2}[f_\alpha m_\alpha+g_\alpha\Omega_\alpha],\tag{D1}$$

where $g_\alpha=T\ln[1+e^{(\mu-\varepsilon_\alpha)/T}]$. First-order perturbation theory gives the energy shift $\delta\varepsilon_\alpha=\delta X_\alpha$ and

$$|\delta\alpha\rangle=\sum_{\beta\neq\alpha}\frac{|\beta\rangle\langle\beta|\delta X|\alpha\rangle}{\varepsilon_\alpha-\varepsilon_\beta}.\tag{D2}$$

Thus, we obtain

$$\begin{aligned}
\tilde{\chi}_{\delta X}&=\sum_\alpha\int\frac{\mathrm{d}^2k}{(2\pi)^2}[f_\alpha\delta m_\alpha+g_\alpha\delta\Omega_\alpha+\delta X_\alpha(f'_\alpha m_\alpha-f_\alpha\Omega_\alpha)],\\
\delta m_\alpha&=\mathrm{Im}[\langle\delta_x\alpha|(H_0^{\mathrm{MF}}-\varepsilon_\alpha)|\partial_y\alpha\rangle+\langle\partial_x\alpha|(H_0^{\mathrm{MF}}-\varepsilon_\alpha)|\delta_y\alpha\rangle+\langle\partial_x\alpha|(\delta X-\delta X_\alpha)|\partial_y\alpha\rangle],\\
\delta\Omega_\alpha&=-2\,\mathrm{Im}[\langle\delta_x\alpha|\partial_y\alpha\rangle+\langle\partial_x\alpha|\delta_y\alpha\rangle],
\end{aligned}\tag{D3}$$

where $|\partial_{x/y}\alpha\rangle=\sum_{\beta\neq\alpha}|\beta\rangle\langle\beta|v_{x/y}|\alpha\rangle/(\varepsilon_\alpha-\varepsilon_\beta)$, and $|\delta_{x/y}\alpha\rangle$ denotes the first-order change of $|\partial_{x/y}\alpha\rangle$, which is given by

$$|\delta_{x/y}\alpha\rangle=\sum_{\beta\neq\alpha}\left[|\delta\beta\rangle\frac{\langle\beta|v_{x/y}|\alpha\rangle}{\varepsilon_\alpha-\varepsilon_\beta}+|\beta\rangle\frac{\langle\delta\beta|v_{x/y}|\alpha\rangle+\langle\beta|\partial_{x/y}(\delta X)|\alpha\rangle+\langle\beta|v_{x/y}|\delta\alpha\rangle}{\varepsilon_\alpha-\varepsilon_\beta}-|\beta\rangle\frac{\langle\beta|v_{x/y}|\alpha\rangle(\delta X_\alpha-\delta X_\beta)}{(\varepsilon_\alpha-\varepsilon_\beta)^2}\right].$$

Appendix E: Two toy models—For the translation-invariant model in Eq. (22), we take $(v,m,\Delta,\lambda,U)=(1,1,0.2,1,2\pi^2)$. The chemical potential is fixed at $\mu=-1.2$ for calculations at both zero and finite fields. Moreover, we introduce a very low temperature, $T=0.01$, to reduce quantum oscillations. The grand potential density at finite temperature is given by

$$\begin{aligned}
\Omega=\frac{1}{\mathcal{A}}\{&\mathrm{tr}_{\mathrm{phys}}[\hat{N}(\hat{h}-\mu)]+\mathrm{tr}_{\mathrm{phys}}[\hat{N}V_{\mathrm{MF}}(\hat{N})]/2\\
&+T\,\mathrm{tr}_{\mathrm{phys}}[\hat{N}\ln\hat{N}+(1-\hat{N})\ln(1-\hat{N})]\}.
\end{aligned}\tag{E1}$$

For the continuum model of $t\mathrm{MoTe}_2$ in Eq. (23), the moiré potential is given by

$$V_l(\mathbf{r}) = -2V \sum_{j=1}^{3} \cos(\mathbf{G}_j \cdot \mathbf{r} + l\psi), \tag{E2}$$

$$T(\mathbf{r}) = -w(1 + e^{-i\mathbf{G}_2 \cdot \mathbf{r}} + e^{i\mathbf{G}_3 \cdot \mathbf{r}}), \tag{E3}$$

where $l = 1$ ($l = -1$) for the bottom (top) layer, $\mathbf{G}_1 = k_\theta[1, 0], \mathbf{G}_2 = k_\theta[-1/2, \sqrt{3}/2]$ are the reciprocal-lattice basis vectors of $t\mathrm{MoTe}_2$, $\mathbf{G}_3 = -\mathbf{G}_1 - \mathbf{G}_2$. The K valleys of the two layers are $\boldsymbol{\kappa}_b = -(2\mathbf{G}_1 + \mathbf{G}_2)/3$ and $\boldsymbol{\kappa}_t = (\mathbf{G}_2 - \mathbf{G}_1)/3$. Here, $k_\theta = 8\pi \sin(\theta/2)/(\sqrt{3}a_0)$ describes the length scale of the system, where a_0 is the lattice constant of MoTe_2, and θ is the twist angle. Adopting the parameters in Ref. [36], we take $(a_0, m, V, \psi, w) = (3.472\text{Å}, 0.62m_e, 8\ \text{meV}, -89.6°, -8.5\ \text{meV})$, where m_e is the bare electron mass, and $\theta = 1.7°$.